14th Australasian Fluid Mechanics Conference
Adelaide University, Adelaide, Australia
10-14 December 2001

A Single Moduled Laser Interferometer for Wall Shear Stress Measurement

N. Nishizawa, M. B. Jones and M. S. Chong

Department of Mechanical and Manufacturing Engineering
University of Melbourne, Victoria, 3010 AUSTRALIA

Abstract

A Laser Interferometer Skin Friction meter (LISF) has been designed and developed for the wall shear stress measurement. Since its introduction in the mid 1970s, the Laser Interferometer has been the focus of a number of studies, however, a number of its major disadvantages have been left unsolved. Conventional LISF and FISF (Fringe Imaging Skin Friction meter) require silicone oil to be applied while there is no airflow. This restriction has created problems in the application and accuracy of the Interferometry system.

As a solution to this problem, a single moduled and single beam Interferometer was designed and built. The original concept of single module design was established by Seto & Hornung [8], and developed by Nishizawa *et al.*[4]. The major change from the previous design was an introduction of a built-in oil injector which enables silicon oil to be deposited upon the surface when a boundary layer is present. Preliminary wall shear stress measurements showed good agreement with the data from the Clauser chart and Preston tube methods. The device was also applied to high Reynolds number turbulent boundary layers as a method which is independent of the law of the wall in determining the wall shear stress.

Introduction

Wall shear stress is one of the critical parameters in fluid mechanics. Aside from its significance in practical applications such as aerodynamical design of vehicles, wall shear stress also plays a key role in the study of the structure of turbulent boundary layers, (see Österlund *et al.*[7] as an example of ongoing discussion about the mean velocity scaling law). Regardless of which scaling law (a logarithmic law of the wall, a power law, or any other modified scaling laws) is used, they usually rely on the wall shear stress. Wall shear stress τ_0 appears in the definition of friction velocity $U_\tau = \sqrt{\tau_0/\rho}$, where ρ is fluid density (alternatively, in the definition, skin friction coefficient $C_f' = 2(U_\tau/U_1)^2$, where U_1 is the free stream velocity).

Despite its importance, accurate measurements of U_τ have been a major problem in boundary layer measurements. Pressure-based measurements, such as the Preston tube, Stanton gauge, or sublayer fence, are popular because of their simple construction and ease of use, however, their accuracy depends on the validity of the law of the wall. As a result of this, they are only valid in zero or weak pressure gradient flows. Velocity profile-based methods, such as the Clauser chart, rely on the validity of the profile model. When trying to examine the *"universal laws"*, none of these methods mentioned above are suitable. A floating element gauge is well known as a direct measurement method, free from any theoretical assumptions. However, this equipment has different problems, such as its sensitivity to vibration and errors in pressure gradient flows. The floating element used at SLTEST [9] was able to overcome these disadvantages. However, its physical dimension is too impractical for application in most wind tunnel experiments.

The optical interferometry method is one of the latest methods of measuring the wall shear stress and was introduced by Tanner and Blows [10] and is a method which is independent of the law of the wall. This is important if one is investigating the validity of the log-law at the wall.

Background Theory

The oil-film method is based on a relation between a time-varying oil film gradient with local skin friction. Tanner and Blows [10] expressed the general relation as follows:

$$\frac{dy}{dx} = \frac{\mu_{oil}}{\tau_0 t}(1+\varepsilon). \tag{1}$$

where dy/dx is the film gradient, μ_{oil} is the oil viscosity, and t is the time. ε is a term which accounts for the effects of pressure gradient and is given as:

$$\varepsilon = \frac{1}{3}\frac{y}{\tau_0}\frac{dp}{dx} + \frac{2}{3}\frac{\mu_{oil}}{t}\int_{p_0}^{p}\frac{1}{\tau_0^2}dp. \tag{2}$$

As can be seen from equation (1), the oil film profile will converge to a linear profile for zero pressure gradient as ε decreases as the film thickness decreases. Thus, the effect of the pressure gradients will become negligible as time increases.

An optical interferometry method is applied to measure the film slope. By applying the laser beam from underneath to an oil film deposited over the flat window, the two reflections, one at the oil-air interface and the other one at the oil-window interface will form one beam. As the second reflection is tilted by the film slope, the resultant mixed beam forms an interference pattern. The relation between the fringe spacing and the film slope is expressed as:

$$\frac{dy}{dx} = \frac{\lambda}{2nD}. \tag{3}$$

where λ is the wavelength of the laser beam (632.8nm for He-Ne Laser) and n is the refractive index of the oil. With FISF, a monochromatic lamp is applied as a light source instead of a laser. Both LISF and FISF were named by Monson *et al.*[3].

From (1) and (3), τ_0 can be expressed as

$$\tau_0 = \frac{2n\mu_{oil}}{\lambda}\frac{D}{t}. \tag{4}$$

A plot of the fringe spacing D versus time t shows that the slope of the graph is directly proportional to τ_0 and the constant of proportionality consists of known constants.

A number of researches on the optical interferometry method have been conducted (see Nishizawa [5] for an overall review). One of the more recent studies was made by Österlund *et al.*[6].

The joint work between the Royal institute of Technology in Sweden and the Illinois Institute of Technology has shown that the laser interferometer results showed reasonable agreement with the so-called "logarithmic friction laws", that is:

$$C_f^{'} = 2\left(\frac{1}{\kappa} ln(R_\theta) + C\right)^{-2} \tag{5}$$

Their experiments have been carried out at R_θ (Reynolds number based on boundary layer momentum thickness) ranging from $2,500$ to $27,000$. In this study, this curve-fit is extended to higher R_θ. The constant C in (5) is also examined.

Experimental Setup

The experiments were carried out in 1) an open-type small wind tunnel, and in 2) a newly-built large boundary layer tunnel. Note the difference in the dimension between the two test sections in figure 1.

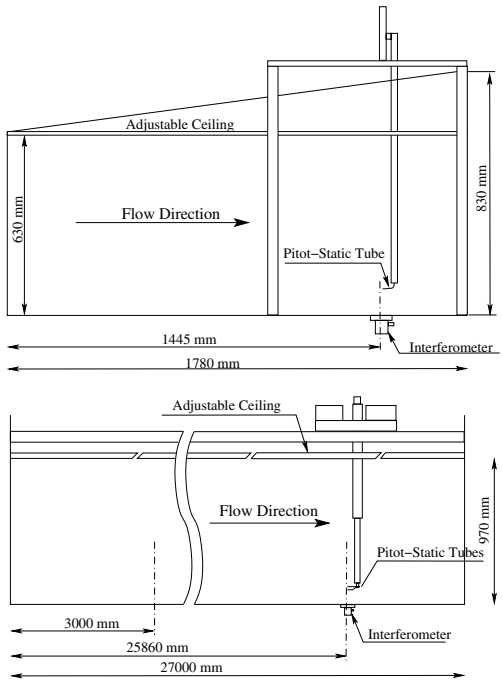

Figure 1: Wind Tunnel Test Sections. Top: Low Reynolds number wind tunnel. Bottom: High Reynolds number wind tunnel (the interferometer was mounted at two different streamwise locations).

In order to create a fully developed turbulent boundary layer, a tripping wire was attached to the leading edge of the test section in both tunnels. Most of the measurements were carried out in zero pressure gradient flows.

Figure 2 shows the newly designed Single-Moduled Laser Interferometer. An oil injection nozzle, which is mounted upstream of a glass window, can be lifted up from the surface like a submarine periscope so as to deliver silicon oil to the boundary layer wall surface. Once the desired amount of oil is delivered, the nozzle can be retracted so that its top surface is flush with the surrounding surface.

The light source is a 20mW He-Ne laser, which is collimated in a beam of approximately 3mm diameter. Silicon oil is favoured because of its low vapour pressure, chemical stability and its

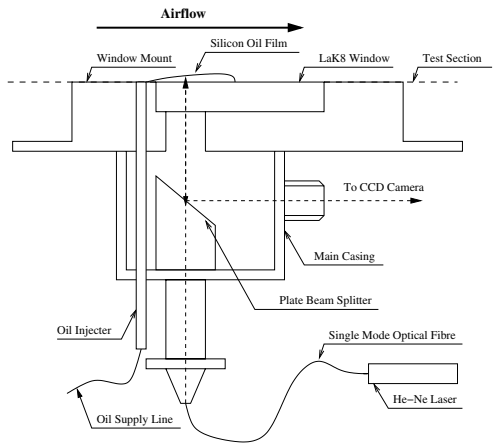

Figure 2: Schematic of Single Moduled Laser Interferometer. The dashed line represents the beam path.

low temperature coefficient of viscosity. The interference images are captured by a CCD camera and recorded on video tape and the images were sampled at a desired rate (one frame per five seconds for most of the cases) to a computer.

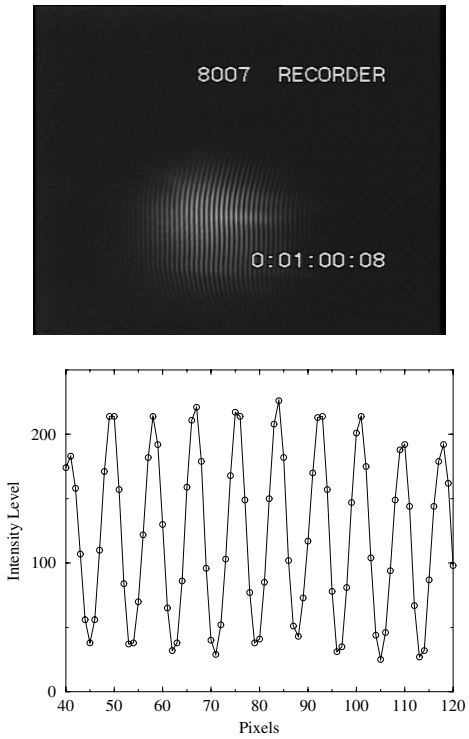

Figure 3: Sample fringe pattern (3mm beam diameter) and its streamwise intensity distribution.

Figure 3 is an example of the captured images. FFT was taken over an area of approximately 1mm by 1mm to obtain a peak frequency. From equation (4), the wall shear stress is obtained by plotting the fringe spacing, that is, the inverse of the peak frequency, versus time t (which gives D/t). Figure 4 shows the plots from different flow cases.

Since this is an adaption of the design by Seto and Hornung [8], the interferometry system adopted by the authors is a single module, apart from the light-source and a CCD camera. This

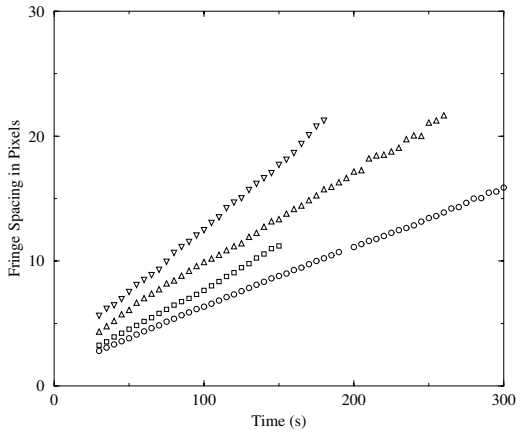

Figure 4: Fringe spacing versus time.

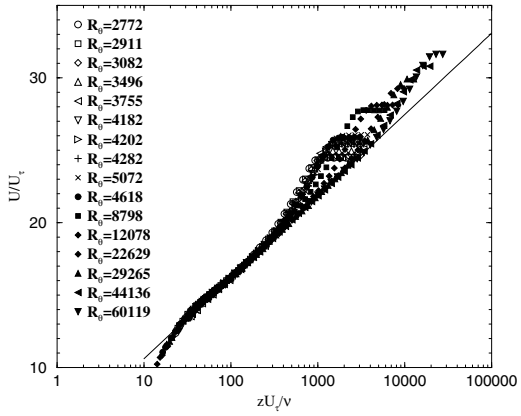

Figure 5: Mean Velocity Profiles. The last six profiles were measured in the high Reynolds number boundary layer tunnel.

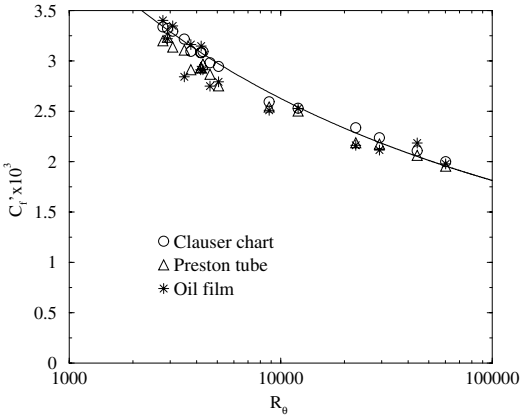

Figure 6: Skin Friction Measurement Result.

requires access to the test section of the wind tunnel only from the floor, while majority of the LISF and FISF systems require double-sided access. This advantage is especially important in external flow applications such as mounting on a moving vehicle surface.

Results and Discussion

For the purpose of testing the functioning of the new oil film interferometer, the device was first installed in a low Reynolds number boundary layer wind tunnel and measurements were taken between $R_\theta = 2772$ and $R_\theta = 5072$. Preliminary measurements were carried out in adverse and favourable pressure gradients and it was confirmed that the oil film method was not affected by the pressure gradients.

Upon completing the tests in the low Reynolds number wind tunnel, the interferometer was installed in the high Reynolds number boundary layer wind tunnel. Oil film measurements were carried out at two different streamwise locations and the results were compared with the Clauser chart and Preston tube methods. Reynolds numbers were selected in order to compare the data taken at different streamwise stations for an investigation reported in a separate paper (see Jones *et al.*[2]).

The skin friction magnitude changed by approximately 700% between the lowest and highest Reynolds numbers measured in the wind tunnels. It was necessary to change the oil viscosity level for this reason. Details of the oil viscosity selection will be discussed later.

Mean Velocity Profiles

Mean velocity profiles from the two wind tunnels can be seen in figure 5. In all flow cases the logarithmic regions are clearly visible. The straight line represents the logarithmic line of $U/U_\tau = \frac{1}{\kappa} ln(zU_\tau/\nu) + A$, with $\kappa = 0.41$ and $A = 5.0$.

Skin Friction Comparison

Figure 6 is the comparison of $C_f^{'}$ value obtained from the three different methods; the Clauser chart, the Preston tube, and the Oil film method. Measurements were carried out at different R_θ values by changing the free stream velocity.

The solid line represents the prediction of $C_f^{'}$ value from R_θ value, based on (5) with $\kappa = 0.41$. A non-linear curve fit to Clauser chart results gives $C = 5.131$.

The $C_f^{'}$ prediction (logarithmic friction law) suggested by Österlund *et al.*[6] should only be used as a reference as its accuracy and reliability have yet to be investigated further. This is mainly because the validity of the formulation (5) relies on the assumption that the boundary layer wake parameter remains invariant with Reynolds number.

Preston tube results gave consistently lower values of $C_f^{'}$ compared to Clauser chart results and the prediction curve. The error was mostly less than 5%.

The high Reynolds number wind tunnel results suggested that the oil film method gives lower values of $C_f^{'}$ to low free stream velocities (or small τ_0). It was found that the $C_f^{'}$ error between oil film method and Clauser chart exceeded 5% when the free stream velocity was below $20m/s$, while the rest of the results were all within the expected error of $\pm 4\%$ (Fernholz *et al.*[1]). Most of the errors are likely to be caused by: 1) temperature and oil viscosity effects, and 2) general behaviour of the film over the boundary layer surface. The results implied that these effects are amplified when τ_0 is small. These points associated with silicon oil film are discussed below.

Oil Film

It is well known that the major difficulties in using the oil film interferometry method come from the properties and behaviour of silicon oil. Although, as mentioned earlier, silicon oil was chosen for this application because of its chemical stability and for the *relatively less* variation in its viscosity with temperature, the magnitude of viscosity variation should be taken into account (see Zilliac [11] for detailed discussion). For this ex-

periment, 50CS (centi-stokes), 100CS, and 200CS silicon oil from Dow Corning 200 Fluid series were used and their viscosity values were measured at three different temperatures (15°C, 22.5°C, and 30°C). Non-linear curve fit to the temperature-viscosity plot of the three points was sufficient to cover the entire temperature range for all experiments. Errors from viscosity estimation are predicted to be approximately $\pm 2\%$ (consultation with Dr.J.Cooper-White at Department of Chemical Engineering, the University of Melbourne).

The viscosity level of the oil is selected based on the sensitivity of the oil to fluctuations in skin friction and the time it takes to form a linear slope. Oil with a high viscosity level requires quite a long time for a linear slope to establish. This increased the chance of the film surface to be contaminated. On the other hand, oil with low viscosity may form too quickly and results in insufficient number of points on the $D-t$ plot (figure 4). Because the magnitude of τ_0 is directly proportional to the gradient of the plot, the accuracy depends on the number of points and the regression coefficient. In addition, the low viscosity oil film will easily be distorted by the velocity fluctuation.

The *traditional problem* of the oil film method, *ie* the film contamination from debris, was not necessarily a significant issue throughout the present experiments. This is primarily because the film surface area was very small and exposure (measurement) time was short compared to the conventional LISF or FISF techniques. It was also possible to re-introduce new oil film over the previous oil film. In some instances dust particles on the oil film were "flushed" and the fringe patterns were re-established.

Occasionally the oil film method gives substantially lower skin friction value because of the surface tension of the silicon oil. A problem arises if there is any gap or step over the measuring surface (an early design of an interferometer by Nishizawa [5] had a $0.2mm$ surface step at $5mm$ downstream of the measuring point, which resulted in 50% lower result of $C_f^{'}$), or if there is an electro-static charge on the surface (Österlund *et al.*[6]). The former effect was avoided by carefully mounting the large window to the boundary layer surface, and the latter issue was effectively solved by re-introducing new oil film over the previous oil film. In many instances the first oil injection "wetted" the surface and the oil film from the succeeding oil injection was used to obtain the required result. Österlund *et al.*[6] had to solve the same problem by using ionized air in their wind tunnel.

Conclusions

A newly designed Laser Interferometer was designed, built, and tested. From the comparison with traditional velocity measurement-based methods, it was found that its accuracy is within reasonable limits.

Acknowledgements

This paper is dedicated to Professor A. E. Perry, who foresaw and believed in the importance and success of this project.

The authors wish to acknowledge the financial assistance of the Australian Research Council.

References

[1] Fernholz, H. H., Janke, G., Schober, M., Wagner, P. M. and Warnack, D., 'New developments and applications of skin-friction measuring techniques', *Meas. Sci. Technol.* 7, 1996, 1396–1409.

[2] Jones, M. B., Nishizawa, N. and Chong, M. S., 'Experimental study of high Reynolds number turbulent boundary layers', *14th AFMC*, 2001

[3] Monson, D. J. and Mateer, G. G., 'Boundary Layer Transition and Global Skin Friction Measurements with an Oil-Fringe Imaging Technique', SAE 932550, Aerotech '93, 1993.

[4] Nishizawa, N., Marusic, I, Perry, A.E. and Hornung, H.G., Measurement of Wall Shear Stress in Turbulent Boundary Layers using an Optical Interferometry Method, *13th AFMC*, 1998, 491–494.

[5] Nishizawa, N., 'Measurement of Wall Shear Stress in Turbulent Boundary Layers using an Optical Interferometry Method', Master's Degree Thesis, The University of Melbourne, 1998.

[6] Österlund, J. M., Johansson, A. V., Nagib, H. M. and Hites, M. H., 'Wall Shear Stress Measurements in High Reynolds Number Boundary Layers from Two Facilities', *AIAA 99-3814*, 1999.

[7] Österlund, J. M., Johansson, A. V. and Nagib, H. M., 'Comment on "A note on the intermediate region in turbulent boundary layers", [Phys. Fluids 12, 2159 (2000)]', *Phys. Fluids.* 12, 2360, 2000.

[8] Seto, J. and Hornung, H., 'Two-Dimensional Skin Friction Measurement Utilizing a Compact Internally-mounted Thin-Liquid Film Skin Friction Meter', AIAA Paper 93-0180, 1993.

[9] Smits, A. J. and Marusic, I.,'High Reynolds Number Flows: A Challenge for Experiments and Simulation', AIAA Paper 99-3530, 1999.

[10] Tanner, L. H. and Blows, L. G., 'A study of the motion of oil films on on surfaces in air flow, with application to the measurement of skin friction', *J. Phys. E:* , 1976, vol.9(3), 194–202.

[11] Zilliac, G. G., 'Further Developments of the Fringe-Imaging Skin Friction Technique', NASA TM 110425, 1996.